

Soft 3D Robots with Hard 2D Materials

Weinan Xu,[†] David H. Gracias^{,†,‡}*

[†]Department of Chemical and Biomolecular Engineering, Johns Hopkins University, Baltimore, Maryland 21218, USA

[‡] Department of Materials Science and Engineering, Johns Hopkins University, Baltimore, Maryland 21218, USA

ABSTRACT

Inspired by biological organisms, soft engineered robots seek to augment the capabilities of rigid robots by providing safe, compliant, and flexible interfaces for human-machine interactions. Soft robots provide significant advantages in applications ranging from pick-and-place, prostheses, wearables, surgical and drug delivery devices. Conventional soft robots are typically composed of elastomers or gels, where changes in material properties such as stiffness or swelling control actuation. However, soft materials have limited electronic and optical performance, mechanical rigidity and stability against environmental damage. Atomically thin two-dimensional layered materials (2DLMs) such as graphene and transition metal dichalcogenides have excellent electrical, optical, mechanical, and barrier properties and have been used to create ultrathin interconnects, transistors, photovoltaics, photocatalysts, and biosensors. Importantly, while 2DLMs have high in-plane stiffness and rigidity, they have high out-of-plane flexibility and are soft from that point of view. Here, we discuss the use of 2DLMs either in their continuous monolayer state or as composites with elastomers and hydrogels to create soft 3D robots, with a focus on origami-inspired approaches. We classify the field, outline major methods, and highlight challenges towards seamless integration of hybrid materials to create multifunctional robots with the characteristics of soft devices.

Soft robots are inspired by the many animals that live on land and in oceans such as caterpillars, worms, octopi and jellyfish.^{1,2} Unlike engineered rigid robots such as pick-and-place assembly arms, drones or self-driving cars, these organisms can conform to surfaces, have continuum material control and low impact forces.³ More recently, the field of soft robotics has been broadened to include soft robots with a fraction of hard components.⁴ These robots are inspired by animals such as millipedes,⁵ fish,⁶ and turtles⁷ which are all soft, but with either exoskeleton, endoskeleton or both (Fig. 1).⁸ Soft robots promise significant advantages as compared to conventional rigid robots, the most important of which is the possibility for humans and machines to collaborate and interact in a safe manner.^{9,10} Other characteristics of soft robots are their simple designs, lightweight, low fabrication cost, accessibility, and power efficiency.^{11,12}

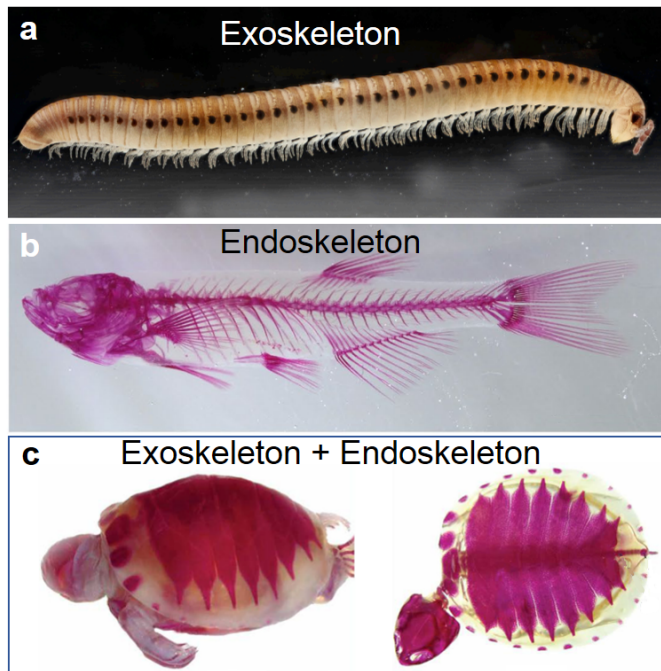


Figure 1. Photograph of a millipede (*Blaniulus guttulatus*) with an exoskeleton structure. Reprinted with permission from ref. 5. Copyright 2015 Elsevier. (b) Optical microscope image of a zebrafish after bone staining, illustrating its endoskeleton structure. Reprinted with permission from ref. 6. Copyright 2018 Nature Publishing Group. (c) Hatchling of a turtle (*Podocnemis expansa*) (left) and with skeletal staining (right) illustrating both endoskeleton bones and carapace. Reprinted with permission from ref. 7.

When considering the types of hard materials to include in soft robots, two-dimensional layered materials (2DLMs), such as graphene and transition metal dichalcogenides (TMDs) have unique characteristics.^{13,14} 2DLMs span the range of functional electrical properties; graphene is a semimetal in its intrinsic state¹⁵ while molybdenum disulfide (MoS_2) is a semiconductor¹⁶ and boron nitride (BN) is an insulator.¹⁷ Therefore, it is possible to fabricate high-performance field-

effect transistors, the critical switching elements in integrated circuits using only 2DLMs.^{18,19} Recent predictions suggest large groups of 2DLMs with magnetic and piezoelectric properties, pointing to the possibility for designing ultrathin actuators.^{20,21} 2DLMs also can interact with light over a broad spectral range of relevance to photodetection and solar energy harvesting.^{22,23} 2DLMs can have extremely high in-plane strength with simultaneous extremely low bending stiffness.^{24,25} For example, the Young's modulus of graphene is estimated to be as high as 1.0 TPa,²⁶ which is hundreds of times higher than that of steel; while its bending stiffness is merely 2.43×10^{-19} N·m²⁷ which is much smaller than a sheet of paper. Indeed, graphene is like "atomic paper" and one can do kirigami with it (Fig. 2a-c).²⁸ Also, 2DLMs have excellent barrier properties,²⁹ for example, graphene is essentially impervious and can encapsulate liquid water even under vacuum.³⁰ Further, 2DLMs are essentially surfaces with extremely high surface area to volume ratios which is advantageous for enhancing interfacial interactions.³¹ For example, graphene has a theoretical surface area of approximately 2630 m²/g which means that it would take less than 1 mg of monolayer graphene to cover the entire human body.³²

The properties of 2DLMs mentioned above make them advantageous for soft robotics.³³ On their own, although very stiff in-plane, 3D structures composed of ultrathin 2DLMs can be soft.³⁴ Previously, graphene was shown to wrap beads, pollen grains, and live cells conformally, like a skin.³⁵ The ability of 2DLMs to conform to different surfaces is of importance to dexterous and universal gripping devices capable of handling diverse objects in unstructured environments.³⁶ Also, due to their atomically thin structure and extremely low bending rigidity, 2DLMs can be easily integrated into a 3D soft matrix without delamination or mechanical failure, which is essential from a reliability perspective.^{37,38} Consequently, they can selectively stiffen soft robots and serve as either an exo- or endo-skeleton. Also, they can augment the functionality of soft robots by facilitating interactions with electromagnetic fields such as by harnessing power from sunlight, or facilitating communication at a distance using lasers.^{39,40}

Recent developments in 3D fabrication such as direct ink writing,⁴¹ stereolithography,⁴² and origami folding,⁴³ facilitate integration of 2DLMs in 3D hybrids.⁴⁴ Herein, we briefly discuss some approaches to create stimuli-responsive structures, actuators and soft robots using 2DLMs. We classify the research field based on the fabrication of reconfigurable architectures with, (a) continuous monolayer graphene, (b) graphene flakes, and (c) other 2DLMs such as MoS₂ and tungsten disulfide (WS₂). Further, we discuss the possibility of fabricating multi-functional soft robots by combining 2DLMs with other novel functional materials, such as nanoparticles or liquid metal,

1. Reconfigurable structures with continuous monolayer graphene

Graphene with high conductivity, large area, and precise layer control is typically formed using chemical vapor deposition (CVD).⁴⁵ Recent developments in micro/nanofabrication and origami/kirigami folding facilitate incorporation of mono or few-layer CVD graphene as the main component to fabricate reconfigurable structures.⁴⁶ One strategy involves the transfer of monolayer CVD graphene onto a stimuli-responsive polymer substrate, for instance, a gradient-crosslinked epoxy (SU-8) film.⁴⁷ SU-8/graphene bilayer films can reversibly fold and unfold upon solvent exchange (Fig. 2d-e), and the incorporation of metal electrodes allows them to function as 3D chemical sensors. Foldable structures with few-layer graphene have also been utilized to create micro/nanoscale, hollow, polyhedral structures capable of volumetric light confinement.⁴⁸ Elsewhere, Teshima et al. have reported the facile assembly of 3D microstructures by transferring monolayer graphene on a poly(chloro-*p*-xylylene) film.⁴⁹ Graphene adheres to the surface of polymeric films *via* noncovalent π – π stacking and the strain gradient causes self-rolling (Fig. 2f-g). These examples illustrate that polymer-2DLMs bilayers provide an attractive and facile strategy to create reconfigurable structures.

However, to utilize the highly flexible characteristics of 2DLMs while still be able to generate well-ordered 3D structures, it is essential to create bilayers with a thickness of a few nanometers or less. We previously reported thermally responsive folding and unfolding of monolayer graphene by surface functionalization using ultrathin polydopamine (PD) and poly(N-isopropylacrylamide) (PNIPAM) brushes.⁵⁰ The functionalized micropatterned graphene can be as thin as 5 nm and self-folds into predesigned 3D structures with reversible deformation that is tunable by temperature (Fig. 2h-k). Importantly, this shape transformation process only requires a slight temperature increase and is compatible with cell culture and many biological processes, and thus can be applied in biosensor and bioelectronic devices.

Atomic layer deposition (ALD) is another attractive strategy to modify graphene without significantly increasing its thickness. For instance, Miskin et al. deposited a 2nm-thick layer of glass on monolayer graphene sheets to create even thinner bimorph actuators that bend with micrometer radii of curvature in response to local pH changes (Fig. 2l).⁵¹ Also, due to low strain relative to fracture thresholds, the high conductivity of graphene is retained in the bent biomorphs. Although these graphene bimorphs are only nanometers thick, they can lift thicker panels, the weight equivalent of a 500-nm-thick silicon chip. With the incorporation of electronic, photonic, and chemical payloads, these basic elements can become a powerful platform for robotics at the micrometer scale.

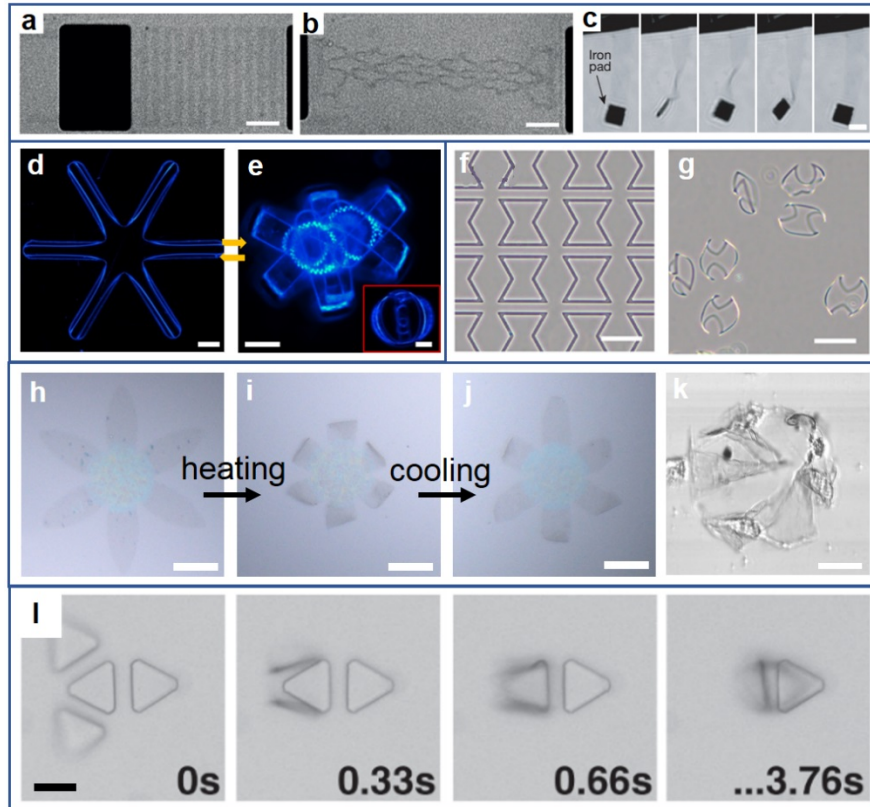


Figure 2. (a-b) Optical microscope images of a graphene in-plane kirigami spring, (a) before, and (b) after being stretched by about 70%. (c) A rotating static magnetic field twists and untwists a long strip of graphene. Scale bars are 10 μ m. Reprinted with permission from ref. 28. Copyright 2015 Nature Publishing Group. (d-e) A flower shaped FLG/SU-8 bilayer in the flat and self-folded states. Scale bars are 200 μ m. Reprinted with permission from ref. 47. Copyright 2015 AIP Publishing LLC. (f-g) Optical microscope image of auxetic shaped graphene-parylene, bilayer patterns before and after folding. Scale bars are 100 μ m. Reprinted with permission from ref. 49. Copyright 2019 American Chemical Society. (h-j) Optical microscope images of a flower shaped thermally-responsive graphene, which can reversibly fold and unfold. Scale bars are 100 μ m. (k) Conformal wrapping of breast cancer cells inside the graphene flower. Scale bar is 20 μ m. Reprinted with permission from ref. 50. Copyright 2017 American Association for the Advancement of Science. (l) Optical microscope images of a tetrahedron shaped graphene-glass bimorph folding upon pH changes. Scale bar is 15 μ m. Reprinted with permission from ref. 51. Copyright 2018 National Academy of Sciences.

2. Reconfigurable structures with graphene flakes

2.1 Graphene flakes dispersed in polymer matrices

2DLMs have an atomically thin structure and abundant surface area, which is a significant advantage for the fabrication of polymer nanocomposites with uniform and predictable properties due to the enhanced interactions between the 2DLMs and the polymer matrix. Several studies describe the incorporation of graphene and graphene oxide (GO) flakes⁵² with polymers to create adaptive nanocomposite structures.^{53,54} Also, nanocomposite films can be patterned with kirigami designs to further increase the variety of reconfigurable structures (Fig. 3a-b).⁵⁵

The dispersion of graphene flakes into an elastomer matrix such as poly(dimethylsiloxane) (PDMS) can significantly alter its mechanical and thermal properties. For instance, Tang et al. have reported near-infrared (NIR) light driven origami assembly using a multi-component composite bilayer film composed of reduced graphene oxide (rGO), thermally expanding microspheres (TEM) and PDMS.⁵⁶ The rGO-TEM-PDMS/PDMS nanocomposite deflects toward the PDMS side upon IR irradiation due to the combined photothermal conversion properties of rGO and the large expansion of the TEMs. The folding angle could be controlled between 0° to 180° by tuning the hinge length to form a wide variety of complex 3D shapes such as a sports car (Fig. 3c).

In another example, a soft robotic system consisting of a bilayer of PDMS/graphene nanoplatelet (GNP) composite and pristine PDMS could be actuated using NIR irradiation due to the differences in the coefficient of thermal expansion (CTE) and modulus of the two layers (Fig. 3d).⁵⁷ This mechanism was used to fabricate an artificial fish whose direction and velocity of motion could be remotely adjusted by light. Interestingly, when the PDMS/GNP layer was illuminated with NIR light from different sides, two different bending behaviors occurred;⁵⁸ which were attributed to differences in temperature gradients along the thickness. The advantage of combining graphene or GO with a polymer in photothermal bilayer actuation is that they have small or even negative CTE's relative to polymers which tend to have relatively high and positive CTE's.

Researchers have also used light to remotely tune the mechanical properties of graphene-based nanocomposites over orders of magnitude. Zhu et al. achieved tunability in composite assemblies of rGO nanoplatelets, nanoclay, and a supramolecular-linked soft polymer.⁵⁹ The rGO nanoplatelets absorb NIR light with rapid and spatiotemporally-controlled heating which breaks the supramolecular bonds leading to a significant localized softening and induction of a stiff to

tough mechanical property transition in the composite. To achieve a more uniform distribution of flakes in a polymer matrix, it is often necessary to functionalize the surface of the 2DLMs. Lee et al. demonstrated that a rationally designed elastin-like polypeptide (ELP) could be used to noncovalently functionalize rGO and form ELP-rGO nanocomposite hydrogels capable of rapid, reversible and tunable NIR light induced actuation.⁶⁰

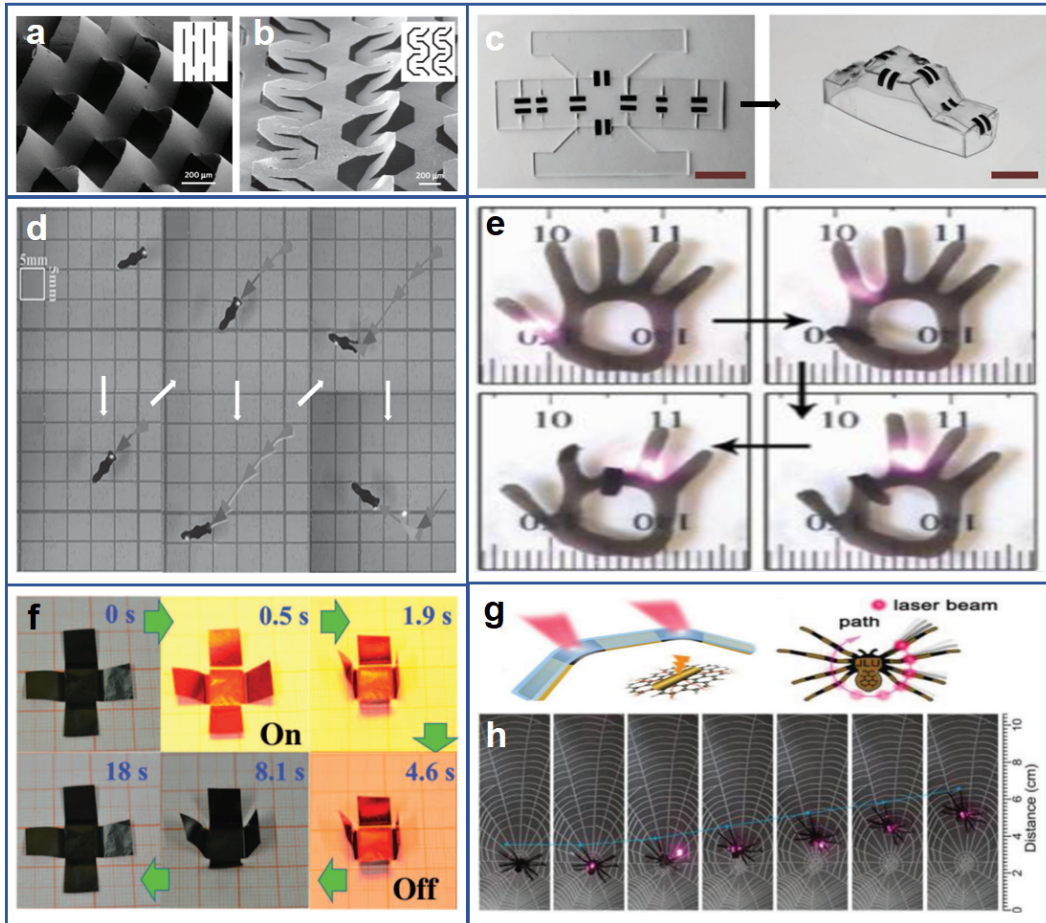


Figure 3. (a-b) Microscale kirigami patterns in GO-PVA nanocomposites, the insets show the corresponding kirigami unit cells. Reprinted with permission from ref. 55. Copyright 2015 Nature Publishing Group. (c) The origami assembly of a 3D sports car from precursor 2D polymer sheets with graphene hinges. The scale bar is 10 mm. Reprinted with permission from ref. 56. Copyright 2017 John Wiley & Sons, Inc. (d) An artificial graphene-PDMS microfish with the capability of forward, backward, and turning motion. Reprinted with permission from ref. 57. Copyright 2014 John Wiley & Sons, Inc. (e) Images of the fingers of a hand-shaped r-GO hydrogel nanocomposite bending and unbending in response to the location of a NIR laser spot. Reprinted with permission from ref. 60. Copyright 2013 American Chemical Society. (f) Time profiles of self-folding movements of a cross-shaped piece of graphene paper before and during NIR light irradiation. Reprinted with permission from ref. 73. Copyright 2015 American Association for the Advancement of Science. (g) Schematic illustration of the patterned artificial muscle, the light-induced deformations can be selectively activated, and enable light-addressable motion manipulation. (h) Light-driven walking of the spider robot: the infrared laser irradiates on the leg, and the local heating induced bending of the leg, leading to the displacement of the gravity center and moving forward. Reprinted with permission from ref. 75. Copyright 2019 John Wiley & Sons, Inc.

Rather than just function as a passive component, the polymer matrix in graphene composites itself can also be adaptive or stimuli-responsive. For instance, Yang et al. used an electric field to induce a spatial gradient of negatively charged GO in a thermally-responsive PNIPAM hydrogel by electrophoresis.⁶¹ Upon NIR light irradiation, the nanocomposite hydrogel exhibited a directional bending deformation and complex actuation. Similarly, Peng et al. have reported a GO/rGO/PNIPAM nanocomposite hydrogel-based deformable actuator, wherein the reduction of GO was achieved electrochemically near the cathode.⁶² The reduction of GO nanosheets leads to hydrogen bond breakage and disassociation between the GO and PNIPAM, altering its swelling characteristics. The researchers were able to demonstrate tunable NIR induced actuation due to differences in the extent and speed of swelling between GO and rGO regions in the nanocomposite GO/rGO/PNIPAM hydrogels. Elsewhere, Wang et al. demonstrated multiple types of actuation from localized bending and site-specific folding to chiral twisting by creating an evaporation-induced laminated and porous bilayer in a GO-clay-PNIPAM hydrogel.⁶³

Liquid crystal elastomers (LCEs) are ordered polymers that can exhibit a reversible shape change in response to heat, light, or solvent exchange.⁶⁴ The performance of LCE actuators is generally limited by their low intrinsic thermal conductivity resulting in low energy transfer and slow response to external stimuli. In order to address this limitation, Yang et al. homogeneously aligned graphene sheets within a nematic LCE matrix by a hot-drawing process, yielding high performance NIR-responsive nanocomposites with reversible mechanical actuation triggered by the nematic-to-isotropic phase transition of the LCE.⁶⁵

Besides NIR light and heat, it is also possible to use chemical stimulation to drive graphene based soft actuators/robotics. For instance, Leeladhar et al. have described multiresponsive soft actuators based on graphene–PDMS nanocomposite/gold bilayers, which display a novel dual mode actuation.⁶⁶ They showed that a 3D tubular structure can be transformed into a two-dimensional sheet upon NIR irradiation illustrating photomechanical actuation. On the other hand, the actuator unscrolls completely and then scrolls in opposite direction upon exposure to acetone or aldehydes, illustrating chemomechanical actuation.

Electrical stimulation is another attractive method to actuate graphene nanocomposites due to the superior conductivity of graphene. For instance, Yang et al. have reported an electrically responsive rGO/poly(2-acrylamido-2-methylpropanesulfonic acid-co-acrylamide)

nanocomposite with enhanced performance.⁶⁷ The rGO nanosheets promote ion transport inside the hydrogel composites resulting in increased osmotic pressure and consequently a larger curvature faster electroresponse times as compared to the pure gel.

By integrating multiple types of responsive polymers into graphene-polymer nanocomposites, researchers have fabricated multi-responsive biomimetic smart structures. Chen et al. reported a bilayer hydrogel actuator with on-off switchable fluorescent color.⁶⁸ The top layer of the hydrogel is a thermoresponsive GO-PNIPAM composite, and the bottom layer is a pH responsive perylene bisimide-functionalized hyperbranched polyethylenimine (PBI-HPEI); the two layers are bonded via macroscopic supramolecular assembly. The actuator can undergo complex shape deformation with changing temperature induced by swelling and shrinkage of the GO-PNIPAM layer, while pH triggers the on-off fluorescence switch in the PBI-HPEI hydrogel layer under the green light irradiation.

2.2 Graphene-polymer composite multilayers

Graphene or GO suspensions can be used to prepare single component paper-like films using vacuum filtration, spin coating, or other deposition methods. These films can be bonded with other polymers to form bimorphs or multilayers that can change their shape or move in a controlled direction when an external stimulus is applied, due to the intrinsic differences in the properties of the layers.⁶⁹ For instance, Yang et al. have reported a bilayer actuator composed of spongy rGO and polyimide.⁷⁰ The actuator produces large deformation, high output force, and dual-stimuli response, due to the electrothermal and photothermal properties of rGO, coupled with the thermal expansion capability of polyimide. Besides the mechanical deformation output, a photo-to-electric generator was also assembled by associating this actuator with a triboelectric element, further enriching the application range of soft actuators. Elsewhere, Deng et al. described laser induced graphene (LIG) structures that were sandwiched between an active polymer poly(vinylidene fluoride) (PVDF) and a passive polymer polyimide (PI).⁷¹ The LIG structures function as a stiff constraining element resisting PVDF expansion and absorbs photo and electrical energy to enhance multi-stimuli responsivity. The researchers demonstrated a series of programmable actuations in the trilayers stimulated by electricity, light, organic vapor, and moisture. Functional polymers with other interesting optical, thermal and electrical properties have also been combined with graphene paper-like films to fabricate reconfigurable structures with multi functionality and superior performance (Fig. 3f).^{72 73 74}

Other types of nanomaterials such as metal nanoparticles or carbon nanotube (CNT) can be co-assembled with graphene to introduce additional bilayer functionality. Sun et al. fabricated an artificial segmented muscle composed of a bilayer with a poly(methyl methacrylate) layer and GO with gold nanorod (Au NR) layer.⁷⁵ The wavelength dependent plasmonic excitation of Au NRs was used to drive photothermal reconfiguration and shape change including the demonstration of a walking spider robot (Fig. 3g-h). Elsewhere, Wang et al. have reported electrothermal actuators based on rGO/Ag particle composites and polyimide.⁷⁶ Hu et al. created an rGO-CNT/PDMS bimorph using a high temperature curing method.⁷⁷ Due to the high thermal conductivity and optical absorption of the rGO-CNT film, and thermal stresses in the bimorph, large magnitude and fast actuation could be achieved. The researchers demonstrated sunlight triggered actuation and a light driven crawler-type robot.

2.3 Wholly carbon structures

For a structure constructed entirely with graphene or GO flakes, it is also possible to introduce structural or property anisotropy by selectively reducing the GO flakes. For instance, Cheng et al. have reported the design and fabrication of graphene/GO fibers with laser-induced locally reduced regions.⁷⁸ On exposure to moisture, these graphene/GO fibers display a complex, predetermined deformation and are promising for woven devices and smart textiles.

Wang et al. fabricated a graphene paper with a gradient rGO/GO structure.⁷⁹ GO exhibits strong water absorption/desorption capability, and rGO is strongly hydrophobic. Both GO and rGO exhibit good photothermal heating effects. These properties are exploited to yield graphene paper with reversible, fast, and controllable mechanical deformation and recovery, in response to moisture, heat, and light. Responsive GO actuator with an integrated self-detecting sensor has also been developed.⁸⁰ The film exhibits an asymmetric surface structure on its two sides, creating a promising actuation ability triggered by multiple stimuli, such as moisture, thermals, and NIR light. Meanwhile, the built-in laser-writing rGO sensor in the film can detect its own deformation in real time.

By bonding a graphene film with a CNT film, a wholly carbon bimorph structure can also be generated with promising application in actuators and soft robotics. For instance, a bilayer paper,⁸¹ composed of adjacent GO and MWCNT layers with the thickness of each layer around 10 μm , was found to curl depending on humidity and/or temperature, which is one of the first cases of a macroscopic graphene-based actuator. Ultrafast and controllable actuators based on GO and oriented CNT were reported.⁸² Multiple types of large-size, reversible deformation in

response to humidity and NIR light were achieved, from two-dimensional directional bending to three-dimensional chiral twisting, all of which are guided by preprogrammed CNT orientations. the remarkable actuation performances allow the wholly carbon actuator to implement diverse complex movements.

3. Reconfigurable structures with other 2DLMs

Besides graphene, there are a wide range of 2DLMs such as BN and TMDs which share the atomically thin nature and ultra-low bending stiffness of graphene. Meanwhile, each of these 2DLMs have their own functionality of relevance to soft robots.

MoS_2 was one of the first TMDs that has been explored for actuator and soft robot applications. For instance, Acerce et al. demonstrated that the dynamic expansion and contraction of electrode films formed by restacking chemically exfoliated nanosheets of metallic MoS_2 on thin plastic substrates can generate substantial mechanical forces (Fig. 4a-c).⁸³ These films are capable of lifting masses that are more than 150 times that of the electrode over several millimeters and for hundreds of cycles. The actuation performance is attributed to the high electrical conductivity of the metallic 1T phase of MoS_2 nanosheets, the elastic modulus of restacked MoS_2 layers (2 to 4 GPa), and fast proton diffusion between the nanosheets.

Elsewhere, Lei et al. used MoS_2 nanocomposite hydrogels as flexible anisotropic actuators with tunable thermo- and photo-responses, in which MoS_2 nanosheets act as the photothermal transduction agents and enable remote and precise control of the actuator locomotion (Fig. 4d).⁸⁴ The anisotropic structure of the hydrogels enables shape deformation and self-wrapping motions under remote control of light or heat.

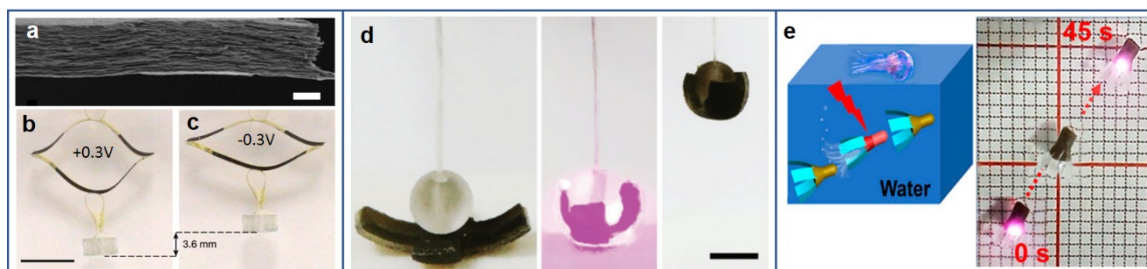


Figure 4. (a) Scanning electron microscope image of a restacked 1T phase 2D MoS_2 film. The scale bar is 2 μm . (b-c) Photographs of the MoS_2 actuator at, (b) its equilibrium position and (c) upon charging of the film, and lifting of a weight by 3.6 mm. The scale bar is 1 cm. Reprinted with permission from ref. 83. Copyright 2017 Nature Publishing Group. (d) A soft actuator based on a MoS_2 hybrid hydrogel grasps a sphere with remote manipulation using a NIR laser. The scale bar is 1 cm. Reprinted with permission from ref. 84. Copyright 2016 Royal Society of Chemistry Journals. (e) Schematic illustration of a jellyfish-inspired swimmer with WS_2 -PNIPAM hydrogel coelom, and swimming behavior driven by actuation of the hydrogel coelom under periodic irradiation. Reprinted with permission from ref. 85. Copyright 2017 American Chemical Society.

Tungsten disulfide (WS_2) has also been used to build proof of concept soft robot with hydrogel. For instance, Zong et al. achieved a prompt actuating behavior by incorporating

alginate-exfoliated WS_2 nanosheets into ice-template-polymerized PNIPAM hydrogels.⁸⁵ A jellyfish-inspired swimmer with the composite hydrogel coelom driven by NIR light was demonstrated (Fig. 4e). The WS_2 nanosheets, on one hand, accelerated water translation within thin cellular membranes by forming interpenetrating networks of alginate and WS_2 nanosheets as water channels. On the other hand, they also enabled super contraction forces of the cellular membranes to drive water out of the cellular pores. This fast and controllable actuation could be further optimized through their pore sizes and compositions of WS_2 nanosheets.

4. Reconfigurable structures with integrated hybrid materials

In order to truly fulfil the promise of soft robotics, the entire range of functions such as sensing, actuation, energy harvesting, decision making, and memory will need to be incorporated within the soft robot. Hence, 2DLMs may need to be augmented with other functional elements such as metal nanostructures. In the latest issue of ACS Nano, Chen et al.⁸⁶ report an approach to produce complex metal oxide (MO) origami structures from paper origami templates via the intercalation of various metal ions during GO-enabled synthesis (Fig. 5a-b). The MO origami structures can be stabilized with an elastomer, and the MO–elastomer origamis could be adapted into multiple actuation systems for the fabrication of MO origami robots. These MO reconfigurable origamis provide an expanded material library for building soft robots with tunable functionality.

Monolayer graphene can also be used as a template for the fabrication of hybrid adaptive systems. We recently demonstrated an approach to decorate surface functionalized monolayer graphene with Ag nanocubes (Ag NCs) (Fig. 5c-e).³⁵ The ultrathin hybrid graphene-Ag NCs structure was shown to wrap soft or irregularly shaped 3D biological samples such as a cancer cell or a pollen grain. This hybrid flexible skin enabled capture, conformal contact and 3D label-free spatially resolved surface analysis of these samples via surface-enhanced Raman spectroscopy (SERS).

The integration of ultrathin 2DLMs with other novel soft materials such as liquid metals (LM) can further broaden the functionality of soft robots.^{87,88} For example, Majidi et al. integrated LM in an elastomer matrix to form a composite with an unprecedented combination of metal-like thermal conductivity, elastic compliance similar to soft biological tissue, and the capability to undergo extreme deformations (Fig. 5f-g).⁸⁹ These properties are enabled by a unique thermal–mechanical coupling that exploits the deformability of the LM inclusions to create thermally conductive pathways *in situ*. These composite materials offer new possibilities for passive heat exchange in stretchable electronics and bioinspired robots. Elsewhere, Chen et al. coated LM droplets with graphene flakes to create highly conductive graphene-coated liquid metal (GLM) droplets.⁹⁰ These GLM droplets function as novel movable, recyclable soft electrical contacts, which is of high relevance for electrically actuated soft robots.

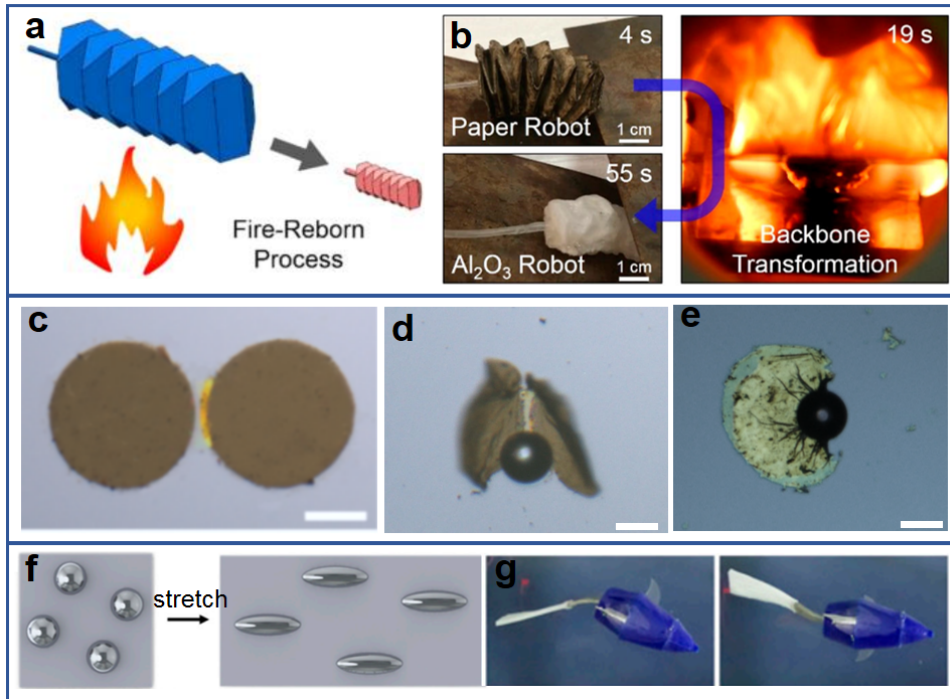


Figure 5. (a) Schematic of the GO-enabled templating synthesis to produce complex MO origami structures from their paper origami templates with high structural replication. (b) Photographs of a pneumatic paper robot transforms into a downsized Al_2O_3 robot via a calcination process. Reprinted with permission from ref. 86. Copyright 2019 American Chemical Society. (c-e) A hybrid graphene-Ag NCs dumbbell structure self fold with temperature increase, and conformally encapsulate a 3D sphere inside. Reprinted with permission from ref. 35. Copyright 2019 American Chemical Society. (f) Schematic illustration of the LM embedded elastomer composite and upon deformation, the LM inclusions and elastomer elongate in the direction of stretching. (g) Forward locomotion of a soft robotic fish composed of a silicone body and caudal fin connected by an LM embedded elastomer actuator. Reprinted with permission from ref. 89. Copyright 2017 National Academy of Sciences.

CONCLUSIONS AND OUTLOOK

In summary, there are many proof-of-concept demonstrations incorporating hard 2DLMs in 3D soft robotic structures. The most basic examples involve the dispersion of graphene or GO flakes in a polymer or stimuli-responsive hydrogel matrix to endow remote actuation by light, electricity or heat. Ultrathin 2DLMs actuators and robots with a thickness less than 10 nm are much less explored and typically require surface functionalization or the deposition of atomically thin inorganic layers.

To further advance the field of soft 3D robots with hard 2DLMs, there are several key challenges that need to be overcome. Firstly, the cost of 2DLMs is still relatively high, especially high-quality films obtained by wafer scale CVD synthesis. Cost is a concern especially for

implementation in macroscale soft robots where may require large quantities of 2DLMs. Secondly, rather than uniformly distributing flakes that function as mechanical enhancement nanofillers in nanocomposites, functional devices based on high quality 2DLMs can be fabricated and integrated into the soft body. For example, field-effect transistors, photodetectors, biosensors based on multiple types of 2DLMs can all be fabricated and integrated into one soft robot to equip it with sensing, communication, and computational capabilities.

Also, the bonding and compatibility of 2DLMs with the soft matrix can be an issue. Due to significant differences in rigidity, hydrophobicity and surface chemistry between the 2DLMs and the polymer matrix, there is a high propensity for failure by delamination, wrinkling, or aggregation. These failure modes will be accelerated during repeated actuation. Further, due to high surface area, the electrical and optical properties of 2DLMs are sensitive to the chemistry of the surrounding environment and will change with temperature, humidity and mechanical deformation. This is a concern for consistency and reproducibility of function.

Despite these challenges, it is clear that the integration of 2DLMs can revolutionize the field of soft robotics due to their unique physical and chemical properties. Importantly, 2DLMs in their mono or few-layer form are inherently soft materials in terms of their capacity to bend and fold, while they can be converted into extremely hard materials in bulk and composite forms. Therefore, they can augment soft-robots in many ways. For instance, they can be used as an exoskeleton to protect the soft robot body from mechanical damage, chemical corrosion, or high temperature.⁹¹ Alternatively, by molding or folding 2DLMs into a well-defined 3D geometry, they can serve as the skeleton for endoskeleton soft robots. When patterned and interconnected, they can form synthetic analogs of the nervous system due to unique electrical properties. Furthermore, when 2DLMs are incorporated both as structural support and a functional element, advanced hybrid soft robots with unprecedented capabilities can be developed.

AUTHOR INFORMATION

Corresponding Author

*E-mail: dgracias@jhu.edu.

ORCID

Weinan Xu: 0000-0002-5352-3302

David H. Gracias: 0000-0003-2735-4725

Notes

The authors declare no competing financial interest.

ACKNOWLEDGMENTS

This work was supported by the Air Force Office of Scientific Research MURI program (FA9550-16-1-0031), and the National Science Foundation (CMMI-1635443 and EFMA-1830893).

REFERENCES

- 1 Wehner, M.; Truby, R. L.; Fitzgerald, D. J.; Mosadegh, B.; Whitesides, G. M.; Lewis, J. A.; Wood, R. J. An Integrated Design and Fabrication Strategy for Entirely Soft, Autonomous Robots. *Nature* **2016**, *536*, 451–455.
- 2 Rus, D.; Tolley, M. T. Design, Fabrication and Control of Soft Robots. *Nature* **2015**, *521*, 467–475.
- 3 Laschi, C.; Mazzolai, B.; Cianchetti, M. Soft Robotics: Technologies and Systems Pushing the Boundaries of Robot Abilities. *Sci. Rob.* **2016**, *1*, eaah3690.
- 4 Manti, M.; Cacucciolo, V.; Cianchetti, M. Stiffening in Soft Robotics: A Review of the State of the Art. *IEEE Rob. Autom. Mag.* **2016**, *23*, 93–106.
- 5 Minelli, A. Genome Evolution: Groping in the Soil Interstices. *Curr. Biol.* **2015**, *25*, R194–R196.
- 6 Sakata-Haga, H.; Uchishiba, M.; Shimada, H.; Tsukada, T.; Mitani, M.; Arikawa, T.; Shoji, H.; Hatta, T. A Rapid and Nondestructive Protocol for Whole-Mount Bone Staining of Small Fish and Xenopus. *Sci. Rep.* **2018**, *8*, 7453.
- 7 Vieira, L. G.; Santos, A. L. Q.; Moura, L. R.; Orpinelli, S. R. T.; Pereira, K. F.; Lima, F. C. Morphology, Development and Heterochrony of the Carapace of Giant Amazon River Turtle *Podocnemis expansa* (Testudines, Podocnemidae). *Pesqui. Vet. Bras.* **2016**, *36*, 436–446.
- 8 Kim, S.; Laschi, C.; Trimmer, B. Soft Robotics: A Bioinspired Evolution in Robotics. *Trends Biotechnol.* **2013**, *31*, 287–294.
- 9 Campbell, S. The Robotics Revolution Will Be Soft: Soft Robotics Proliferate-Along with Their Sources of Inspiration. *IEEE Pulse* **2018**, *9*, 19–24.
- 10 Whitesides, G. M. Soft Robotics. *Angew. Chem. Int. Ed Engl.* **2018**, *57*, 4258–4273.
- 11 Rich, S. I.; Wood, R. J.; Majidi, C. Untethered Soft Robotics. *Nat. Electron.* **2018**, *1*, 102–112.
- 12 Bartlett, N. W.; Tolley, M. T.; Overvelde, J. T. B.; Weaver, J. C.; Mosadegh, B.; Bertoldi, K.; Whitesides, G. M.; Wood, R. J. SOFT ROBOTICS. A 3D-Printed, Functionally Graded Soft Robot Powered by Combustion. *Science* **2015**, *349*, 161–165.
- 13 Novoselov, K. S.; Fal'ko, V. I.; Colombo, L.; Gellert, P. R.; Schwab, M. G.; Kim, K. A Roadmap for Graphene. *Nature* **2012**, *490*, 192–200.
- 14 Novoselov, K. S.; Mishchenko, A.; Carvalho, A.; Castro Neto, A. H. 2D Materials and van Der Waals Heterostructures. *Science* **2016**, *353*, aac9439.
- 15 Das, A.; Pisana, S.; Chakraborty, B.; Piscanec, S.; Saha, S. K.; Waghmare, U. V.; Novoselov, K. S.; Krishnamurthy, H. R.; Geim, A. K.; Ferrari, A. C.; Sood, A. K. Monitoring Dopants by Raman Scattering in an Electrochemically Top-Gated Graphene Transistor. *Nat. Nanotechnol.* **2008**, *3*, 210–215.
- 16 Radisavljevic, B.; Radenovic, A.; Brivio, J.; Giacometti, V.; Kis, A. Single-Layer MoS₂ Transistors. *Nat. Nanotechnol.* **2011**, *6*, 147–150.
- 17 Dean, C. R.; Young, A. F.; Meric, I.; Lee, C.; Wang, L.; Sorgenfrei, S.; Watanabe, K.; Taniguchi, T.; Kim, P.; Shepard, K. L.; Hone, J. Boron Nitride Substrates for High-Quality Graphene Electronics. *Nat. Nanotechnol.* **2010**, *5*, 722–726.
- 18 Roy, T.; Tosun, M.; Kang, J. S.; Sachid, A. B.; Desai, S. B.; Hettick, M.; Hu, C. C.; Javey, A. Field-Effect Transistors Built from All Two-Dimensional Material Components. *ACS Nano* **2014**, *8*, 6259–6264.
- 19 Fiori, G.; Bonaccorso, F.; Iannaccone, G.; Palacios, T.; Neumaier, D.; Seabaugh, A.; Banerjee, S. K.; Colombo, L. Electronics Based on Two-Dimensional Materials. *Nat. Nanotechnol.* **2014**, *9*, 768–779.
- 20 Cheon, G.; Duerloo, K.-A. N.; Sendek, A. D.; Porter, C.; Chen, Y.; Reed, E. J. Data Mining for New Two- and One-Dimensional Weakly Bonded Solids and Lattice-Commensurate Heterostructures. *Nano Lett.* **2017**, *17*, 1915–1923.
- 21 Wu, W.; Wang, L.; Li, Y.; Zhang, F.; Lin, L.; Niu, S.; Chenet, D.; Zhang, X.; Hao, Y.; Heinz, T. F.; Hone, J.; Wang, Z. L. Piezoelectricity of Single-Atomic-Layer MoS₂ for Energy Conversion and Piezotronics. *Nature* **2014**, *514*, 470–474.
- 22 Lopez-Sanchez, O.; Lembke, D.; Kayci, M.; Radenovic, A.; Kis, A. Ultrasensitive Photodetectors Based on Monolayer MoS₂. *Nat. Nanotechnol.* **2013**, *8*, 497–501.
- 23 Yin, Z.; Zhu, J.; He, Q.; Cao, X.; Tan, C.; Chen, H.; Yan, Q.; Zhang, H. Graphene-Based Materials for Solar Cell Applications. *Adv. Energy Mater.* **2014**, *4*, 1300574.
- 24 Akinwande, D.; Brennan, C. J.; Scott Bunch, J.; Egberts, P.; Felts, J. R.; Gao, H.; Huang, R.; Kim, J.-S.; Li, T.; Li, Y.; Liechti, K. M.; Lu, N.; Park, H. S.; Reed, E. J.; Wang, P.; Yakobson, B. I.; Zhang, T.; Zhang, Y. W.; Zhou, Y.; Zhuo, Y. A Review on Mechanics and Mechanical Properties of 2D materials-Graphene and beyond. *Extreme Mech. Lett.* **2017**, *13*, 42–77.

25 Kim, S. J.; Choi, K.; Lee, B.; Kim, Y.; Hong, B. H. Materials for Flexible, Stretchable Electronics: Graphene and 2D Materials. *Ann. Rev. Mater. Res.* **2015**, *45*, 63–84.

26 Lee, C.; Wei, X.; Kysar, J. W.; Hone, J. Measurement of the Elastic Properties and Intrinsic Strength of Monolayer Graphene. *Science* **2008**, *321*, 385–388.

27 Wei, Y.; Wang, B.; Wu, J.; Yang, R.; Dunn, M. L. Bending Rigidity and Gaussian Bending Stiffness of Single-Layered Graphene. *Nano Lett.* **2013**, *13*, 26–30.

28 Blees, M. K.; Barnard, A. W.; Rose, P. A.; Roberts, S. P.; McGill, K. L.; Huang, P. Y.; Ruyack, A. R.; Kevek, J. W.; Kobrin, B.; Muller, D. A.; McEuen, P. L. Graphene Kirigami. *Nature* **2015**, *524*, 204–207.

29 Joshi, R. K.; Carbone, P.; Wang, F. C.; Kravets, V. G.; Su, Y.; Grigorieva, I. V.; Wu, H. A.; Geim, A. K.; Nair, R. R. Precise and Ultrafast Molecular Sieving through Graphene Oxide Membranes. *Science* **2014**, *343*, 752–754.

30 Yuk, J. M.; Park, J.; Ercius, P.; Kim, K.; Hellebusch, D. J.; Crommie, M. F.; Lee, J. Y.; Zettl, A.; Alivisatos, A. P. High-Resolution EM of Colloidal Nanocrystal Growth Using Graphene Liquid Cells. *Science* **2012**, *336*, 61–64.

31 Stankovich, S.; Dikin, D. A.; Dommett, G. H. B.; Kohlhaas, K. M.; Zimney, E. J.; Stach, E. A.; Piner, R. D.; Nguyen, S. T.; Ruoff, R. S. Graphene-Based Composite Materials. *Nature* **2006**, *442*, 282–286.

32 Stoller, M. D.; Park, S.; Zhu, Y.; An, J.; Ruoff, R. S. Graphene-based ultracapacitors. *Nano Lett.* **2008**, *8*, 3498–3502.

33 Yu, X.; Cheng, H.; Zhang, M.; Zhao, Y.; Qu, L.; Shi, G. Graphene-Based Smart Materials. *Nat. Rev. Mater.* **2017**, *2*, 17046.

34 Sun, H.; Xu, Z.; Gao, C. Multifunctional, Ultra-Flyweight, Synergistically Assembled Carbon Aerogels. *Adv. Mater.* **2013**, *25*, 2554–2560.

35 Xu, W.; Paidi, S. K.; Qin, Z.; Huang, Q.; Yu, C.-H.; Pagaduan, J. V.; Buehler, M. J.; Barman, I.; Gracias, D. H. Self-Folding Hybrid Graphene Skin for 3D Biosensing. *Nano Lett.* **2019**, *19*, 1409–1417.

36 Brown, E.; Rodenberg, N.; Amend, J.; Mozeika, A.; Steltz, E.; Zakin, M. R.; Lipson, H.; Jaeger, H. M. Universal Robotic Gripper Based on the Jamming of Granular Material. *Proc. Natl. Acad. Sci. U.S.A.* **2010**, *107*, 18809–18814.

37 Ramanathan, T.; Abdala, A. A.; Stankovich, S.; Dikin, D. A.; Herrera-Alonso, M.; Piner, R. D.; Adamson, D. H.; Schniepp, H. C.; Chen, X.; Ruoff, R. S.; Nguyen, S. T.; Aksay, I. A.; Prud'Homme R. K.; Brinson, L. C. Functionalized Graphene Sheets for Polymer Nanocomposites. *Nat. Nanotechnol.* **2008**, *3*, 327–331.

38 Hu, K.; Kulkarni, D. D.; Choi, I.; Tsukruk, V. V. Graphene-Polymer Nanocomposites for Structural and Functional Applications. *Progress in Polymer Science* **2014**, *39*, 1934–1972.

39 Mak, K. F.; Shan, J. Photonics and Optoelectronics of 2D Semiconductor Transition Metal Dichalcogenides. *Nat. Photonics* **2016**, *10*, 216–226.

40 Sun, Z.; Martinez, A.; Wang, F. Optical Modulators with 2D Layered Materials. *Nat. Photonics* **2016**, *10*, 227–238.

41 García-Tuñon, E.; Barg, S.; Franco, J.; Bell, R.; Eslava, S.; D'Elia, E.; Maher, R. C.; Guitian, F.; Saiz, E. Printing in Three Dimensions with Graphene. *Adv. Mater.* **2015**, *27*, 1688–1693.

42 Manapat, J. Z.; Chen, Q.; Ye, P.; Advincula, R. C. 3D Printing of Polymer Nanocomposites via Stereolithography. *Macromol. Mater. Eng.* **2017**, *302*, 1600553.

43 Shenoy, V. B.; Gracias, D. H. Self-Folding Thin-Film Materials: From Nanopolyhedra to Graphene Origami. *MRS Bull.* **2012**, *37*, 847–854.

44 Xu, W.; Kwok, K. S.; Gracias, D. H. Ultrathin Shape Change Smart Materials. *Acc. Chem. Res.* **2018**, *51*, 436–444.

45 Zhang, Y.; Zhang, L.; Zhou, C. Review of Chemical Vapor Deposition of Graphene and Related Applications. *Acc. Chem. Res.* **2013**, *46*, 2329–2339.

46 Zhu, S.-E.; Shabani, R.; Rho, J.; Kim, Y.; Hong, B. H.; Ahn, J.-H.; Cho, H. J. Graphene-Based Bimorph Microactuators. *Nano Lett.* **2011**, *11*, 977–981.

47 Deng, T.; Yoon, C.; Jin, Q.; Li, M.; Liu, Z.; Gracias, D. H. Self-Folding Graphene-Polymer Bilayers. *Appl. Phys. Lett.* **2015**, *106*, 203108.

48 Joung, D.; Nemilentsau, A.; Agarwal, K.; Dai, C.; Liu, C.; Su, Q.; Li, J.; Low, T.; Koester, S. J.; Cho, J.-H. Self-Assembled Three-Dimensional Graphene-Based Polyhedrons Inducing Volumetric Light Confinement. *Nano Lett.* **2017**, *17*, 1987–1994.

49 Teshima, T. F.; Henderson, C. S.; Takamura, M.; Ogawa, Y.; Wang, S.; Kashimura, Y.; Sasaki, S.; Goto, T.; Nakashima, H.; Ueno, Y. Self-Folded Three-Dimensional Graphene with a Tunable Shape and Conductivity. *Nano Lett.* **2019**, *19*, 461–470.

50 Xu, W.; Qin, Z.; Chen, C.-T.; Kwag, H. R.; Ma, Q.; Sarkar, A.; Buehler, M. J.; Gracias, D. H. Ultrathin Thermoresponsive Self-Folding 3D Graphene. *Sci. Adv.* **2017**, *3*, e1701084.

51 Miskin, M. Z.; Dorsey, K. J.; Bircan, B.; Han, Y.; Muller, D. A.; McEuen, P. L.; Cohen, I. Graphene-Based Bimorphs for Micron-Sized, Autonomous Origami Machines. *Proc. Natl. Acad. Sci. U. S. A.* **2018**, *115*, 466–470.

52 Yu, L.; Yu, H. Light-Powered Tumbler Movement of Graphene Oxide/polymer Nanocomposites. *ACS Appl. Mater. Interfaces* **2015**, *7*, 3834–3839.

53 Shi, K.; Liu, Z.; Wei, Y.-Y.; Wang, W.; Ju, X.-J.; Xie, R.; Chu, L.-Y. Near-Infrared Light-Responsive Poly(N-isopropylacrylamide)/Graphene Oxide Nanocomposite Hydrogels with Ultrahigh Tensibility. *ACS Appl. Mater. Interfaces* **2015**, *7*, 27289–27298.

54 Zhao, Q.; Liang, Y.; Ren, L.; Yu, Z.; Zhang, Z.; Ren, L. Bionic Intelligent Hydrogel Actuators with Multimodal Deformation and Locomotion. *Nano Energy* **2018**, *51*, 621–631.

55 Shyu, T. C.; Damasceno, P. F.; Dodd, P. M.; Lamoureux, A.; Xu, L.; Shlian, M.; Shtein, M.; Glotzer, S. C.; Kotov, N. A. A Kirigami Approach to Engineering Elasticity in Nanocomposites through Patterned Defects. *Nat. Mater.* **2015**, *14*, 785–789.

56 Tang, Z.; Gao, Z.; Jia, S.; Wang, F.; Wang, Y. Graphene-Based Polymer Bilayers with Superior Light-Driven Properties for Remote Construction of 3D Structures. *Adv. Sci.* **2017**, *4*, 1600437.

57 Jiang, W.; Niu, D.; Liu, H.; Wang, C.; Zhao, T.; Yin, L.; Shi, Y.; Chen, B.; Ding, Y.; Lu, B. Photoresponsive Soft-Robotic Platform: Biomimetic Fabrication and Remote Actuation. *Adv. Funct. Mater.* **2014**, *24*, 7598–7604.

58 Niu, D.; Jiang, W.; Liu, H.; Zhao, T.; Lei, B.; Li, Y.; Yin, L.; Shi, Y.; Chen, B.; Lu, B. Reversible Bending Behaviors of Photomechanical Soft Actuators Based on Graphene Nanocomposites. *Sci. Rep.* **2016**, *6*, 27366.

59 Zhu, B.; Noack, M.; Merindol, R.; Barner-Kowollik, C.; Walther, A. Light-Adaptive Supramolecular Nacre-Mimetic Nanocomposites. *Nano Lett.* **2016**, *16*, 5176–5182.

60 Wang, E.; Desai, M. S.; Lee, S.-W. Light-Controlled Graphene-Elastin Composite Hydrogel Actuators. *Nano Lett.* **2013**, *13*, 2826–2830.

61 Yang, Y.; Tan, Y.; Wang, X.; An, W.; Xu, S.; Liao, W.; Wang, Y. Photothermal Nanocomposite Hydrogel Actuator with Electric-Field-Induced Gradient and Oriented Structure. *ACS Appl. Mater. Interfaces* **2018**, *10*, 7688–7692.

62 Peng, X.; Jiao, C.; Zhao, Y.; Chen, N.; Wu, Y.; Liu, T.; Wang, H. Thermoresponsive Deformable Actuators Prepared by Local Electrochemical Reduction of Poly(N-isopropylacrylamide)/Graphene Oxide Hydrogels. *ACS Appl. Nano Mater.* **2018**, *1*, 1522–1530.

63 Wang, J.; Wang, J.; Chen, Z.; Fang, S.; Zhu, Y.; Baughman, R. H.; Jiang, L. Tunable, Fast, Robust Hydrogel Actuators Based on Evaporation-Programmed Heterogeneous Structures. *Chem. Mater.* **2017**, *29*, 9793–9801.

64 Ware, T. H.; McConney, M. E.; Wie, J. J.; Tondiglia, V. P.; White, T. J. Voxelated Liquid Crystal Elastomers. *Science* **2015**, *347*, 982–984.

65 Yang, Y.; Zhan, W.; Peng, R.; He, C.; Pang, X.; Shi, D.; Jiang, T.; Lin, Z. Graphene-Enabled Superior and Tunable Photomechanical Actuation in Liquid Crystalline Elastomer Nanocomposites. *Adv. Mater.* **2015**, *27*, 6376–6381.

66 Leeladhar; Leeladhar; Singh, J. P. Photomechanical and Chemomechanical Actuation Behavior of Graphene–Poly(dimethylsiloxane)/Gold Bilayer Tube for Multimode Soft Grippers and Volatile Organic Compounds Detection Applications. *ACS Appl. Mater. Interfaces* **2018**, *10*, 33956–33965.

67 Yang, C.; Liu, Z.; Chen, C.; Shi, K.; Zhang, L.; Ju, X.-J.; Wang, W.; Xie, R.; Chu, L.-Y. Reduced Graphene Oxide-Containing Smart Hydrogels with Excellent Electro-Response and Mechanical Properties for Soft Actuators. *ACS Appl. Mater. Interfaces* **2017**, *9*, 15758–15767.

68 Ma, C.; Lu, W.; Yang, X.; He, J.; Le, X.; Wang, L.; Zhang, J.; Serpe, M. J.; Huang, Y.; Chen, T. Bioinspired Anisotropic Hydrogel Actuators with On-Off Switchable and Color-Tunable Fluorescence Behaviors. *Adv. Funct. Mater.* **2018**, *28*, 1704568.

69 Leeladhar; Raturi, P.; Singh, J. P. Sunlight-Driven Eco-Friendly Smart Curtain Based on Infrared Responsive Graphene Oxide-Polymer Photoactuators. *Sci. Rep.* **2018**, *8*, 3687.

70 Yang, L.; Qi, K.; Chang, L.; Xu, A.; Hu, Y.; Zhai, H.; Lu, P. A Powerful Dual-Responsive Soft Actuator and Photo-to-Electric Generator Based on Graphene Micro-Gasbags for Bioinspired Applications. *J. Mater. Chem. B* **2018**, *6*, 5031–5038.

71 Deng, H.; Zhang, C.; Su, J.-W.; Xie, Y.; Zhang, C.; Lin, J. Bioinspired Multi-Responsive Soft Actuators Controlled by Laser Tailored Graphene Structures. *J. Mater. Chem. B* **2018**, *6*, 5415–5423.

72 Liang, J.; Huang, L.; Li, N.; Huang, Y.; Wu, Y.; Fang, S.; Oh, J.; Kozlov, M.; Ma, Y.; Li, F.; Baughman, R.; Chen, Y. Electromechanical Actuator with Controllable Motion, Fast Response Rate, and High-Frequency Resonance Based on Graphene and Polydiacetylene. *ACS Nano* **2012**, *6*, 4508–4519.

73 Mu, J.; Hou, C.; Wang, H.; Li, Y.; Zhang, Q.; Zhu, M. Origami-Inspired Active Graphene-Based Paper for Programmable Instant Self-Folding Walking Devices. *Sci. Adv.* **2015**, *1*, e1500533.

74 Yang, Y.; Zhang, M.; Li, D.; Shen, Y. Graphene-Based Light-Driven Soft Robot with Snake-Inspired Concertina and Serpentine Locomotion. *Adv. Mater. Technol.* **2019**, *4*, 1800366.

75 Han, B.; Zhang, Y.; Zhu, L.; Li, Y.; Ma, Z.; Liu, Y.; Zhang, X.; Cao, X.; Chen, Q.; Qiu, C.; Sun, H. Plasmonic-Assisted Graphene Oxide Artificial Muscles. *Adv. Mater.* **2019**, *31*, 1806386.

76 Wang, Q.; Li, Y.-T.; Zhang, T.-Y.; Wang, D.-Y.; Tian, Y.; Yan, J.-C.; Tian, H.; Yang, Y.; Yang, F.; Ren, T.-L. Low-Voltage, Large-Strain Soft Electrothermal Actuators Based on Laser-Reduced Graphene oxide/Ag Particle Composites. *Appl. Phys. Lett.* **2018**, *112*, 133902.

77 Hu, Y.; Wu, G.; Lan, T.; Zhao, J.; Liu, Y.; Chen, W. A Graphene-Based Bimorph Structure for Design of High Performance Photoactuators. *Adv. Mater.* **2015**, *27*, 7867–7873.

78 Cheng, H.; Liu, J.; Zhao, Y.; Hu, C.; Zhang, Z.; Chen, N.; Jiang, L.; Qu, L. Graphene Fibers with Predetermined Deformation as Moisture-Triggered Actuators and Robots. *Angew. Chem. Int. Ed Engl.* **2013**, *52*, 10482–10486.

79 Mu, J.; Hou, C.; Zhu, B.; Wang, H.; Li, Y.; Zhang, Q. A Multi-Responsive Water-Driven Actuator with Instant and Powerful Performance for Versatile Applications. *Sci. Rep.* **2015**, *5*, 9503.

80 Cheng, H.; Zhao, F.; Xue, J.; Shi, G.; Jiang, L.; Qu, L. One Single Graphene Oxide Film for Responsive Actuation. *ACS Nano* **2016**, *10*, 9529–9535.

81 Park, S.; An, J.; Suk, J. W.; Ruoff, R. S. Graphene-Based Actuators. *Small* **2010**, *6*, 210–212.

82 Li, H.; Wang, J. Ultrafast yet Controllable Dual-Responsive All-Carbon Actuators for Implementing Unusual Mechanical Movements. *ACS Appl. Mater. Interfaces* **2019**, *11*, 10218–10225.

83 Acerce, M.; Akdoğan, E. K.; Chhowalla, M. Metallic Molybdenum Disulfide Nanosheet-Based Electrochemical Actuators. *Nature* **2017**, *549*, 370–373.

84 Lei, Z.; Zhu, W.; Sun, S.; Wu, P. MoS₂-Based Dual-Responsive Flexible Anisotropic Actuators. *Nanoscale* **2016**, *8*, 18800–18807.

85 Zong, L.; Li, X.; Han, X.; Lv, L.; Li, M.; You, J.; Wu, X.; Li, C. Activation of Actuating Hydrogels with WS₂ Nanosheets for Biomimetic Cellular Structures and Steerable Prompt Deformation. *ACS Appl. Mater. Interfaces* **2017**, *9*, 32280–32289.

86 Yang, H.; Yeow, B. S.; Chang, T.-H.; Li, K.; Fu, F.; Ren, H.; Chen, P.-Y. Graphene Oxide-Enabled Synthesis of Metal Oxide Origamis for Soft Robotics. *ACS Nano* **2019**.

87 Dickey, M. D. Stretchable and Soft Electronics Using Liquid Metals. *Adv. Mater.* **2017**, *29*.

88 Eaker, C. B.; Dickey, M. D. Liquid Metal Actuation by Electrical Control of Interfacial Tension. *Appl. Phys. Rev.* **2016**, *3*, 031103.

89 Bartlett, M. D.; Kazem, N.; Powell-Palm, M. J.; Huang, X.; Sun, W.; Malen, J. A.; Majidi, C. High Thermal Conductivity in Soft Elastomers with Elongated Liquid Metal Inclusions. *Proc. Natl. Acad. Sci. U. S. A.* **2017**, *114*, 2143–2148.

90 Chen, Y.; Zhou, T.; Li, Y.; Zhu, L.; Handschuh-Wang, S.; Zhu, D.; Zhou, X.; Liu, Z.; Gan, T.; Zhou, X. Robust Fabrication of Nonstick, Noncorrosive, Conductive Graphene-Coated Liquid Metal Droplets for Droplet-Based, Floating Electrodes. *Adv. Funct. Mater.* **2018**, *28*, 1706277.

91 Xu, X.; Zhang, Q.; Hao, M.; Hu, Y.; Lin, Z.; Peng, L.; Wang, T.; Ren, X.; Wang, C.; Zhao, Z.; Wan, C.; Fei, H.; Wang, L.; Zhu, J.; Sun, H.; Chen, W.; Du, T.; Deng, B.; Cheng, G. J.; Shakir, I. *et al.* Double-Negative-Index Ceramic Aerogels for Thermal Superinsulation. *Science* **2019**, *363*, 723–727.